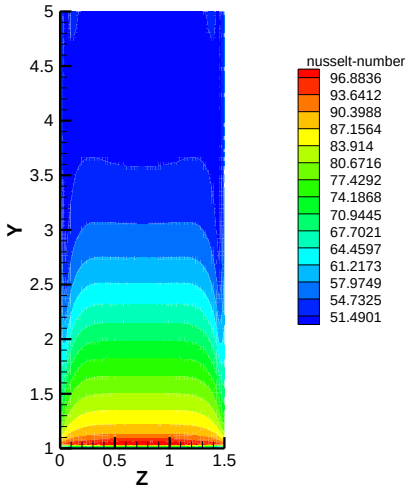

Figure 11. Nusselt number distribution on the vertical heated wall for q=600 W/m^2.

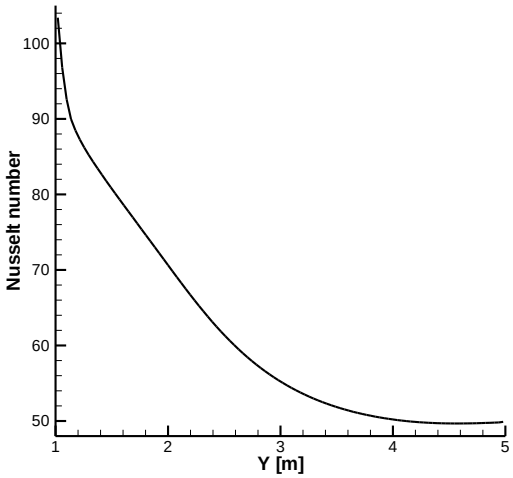

Figure 12. Local Nusselt number on the heated wall, at the mid-channel section (Z=0.75 m) for q=600 W/m^2.

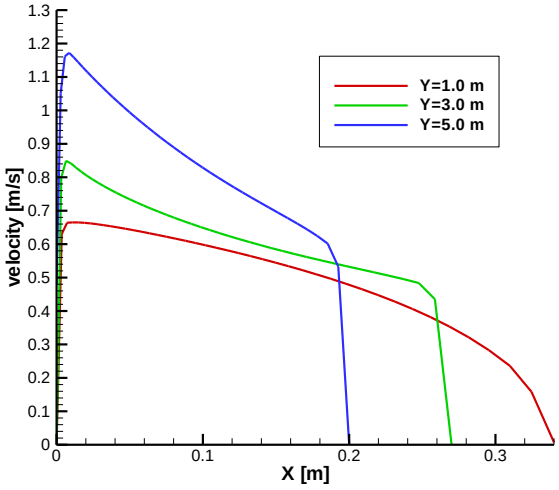

Figure13. Velocity magnitude profile in the channel spacing, at the mid-channel section (Z=0.75 m) and several heights for q=600 W/m^2.

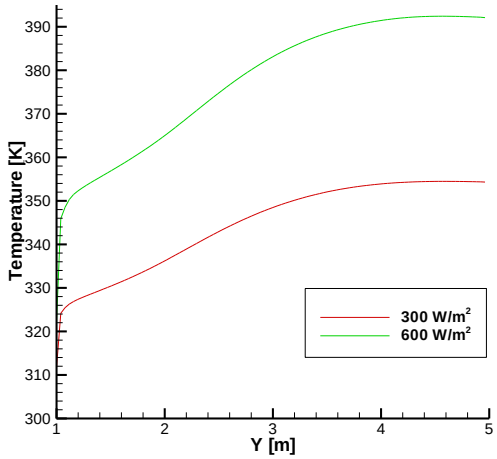

Figure 14. Comparison of centerline heated wall temperature.

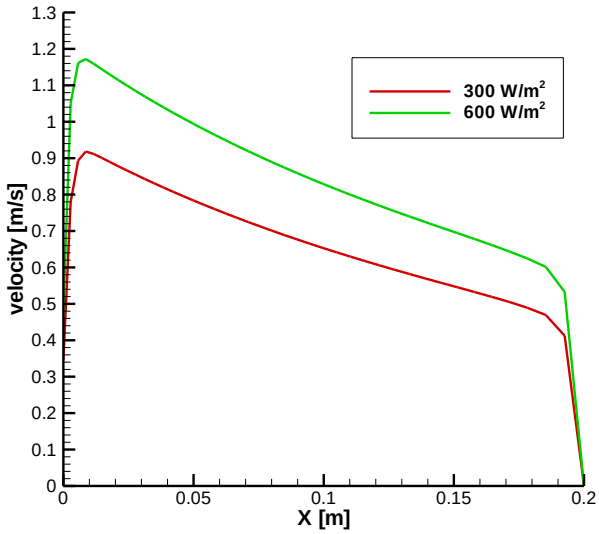

Figure15. Comparison of outlet magnitude velocity.

Table 5. Comparison between the significant quantities for q=300 and 600 W/m^2.

	H= 1.0 m	H= 1.0 m
Heat flux [W/m^2]	300	600
Average Nusselt number	53.8	60.9
Mass flow rate [g/s]	227	289
V_{max} [m/s]	0.92	1.18
T_{max} [K]	357	395

4.2 Geometry parameters effect

In this paragraph, the geometry effect on solar chimney is evaluated considering a channel with vertical parallel walls. The thickness is equal to 0.20 m while all other parameters are equal to the previous case.

Figures 16 shows the field of temperature of vertical surface in case of heat flux equal to 300 W/m^2. Also in this case it is noted that the temperature increases from bottom to top for the progressive heating of the air, assuming a uniform value, about 350 K, at mid-wall. The air temperature, in the channel, grows from bottom to up, presenting the highest values near the heated wall, Fig. 17.

The distribution of the Nusselt number on the vertical surface is reported in Fig. 18, it is noted that it decreases from the bottom upwards due to the reduction of the convective heat transfer. Fig. 19 reports the local Nusselt number profile along the heated wall centerline and its value varies from 117 to 42. Average Nusselt number is equal to 52.9. The maximum air velocity increases from bottom to up, in the solar chimney, due to air heating close to the heated wall, as reported in Fig. 19. In figure velocity profiles, for three different values of Y, are given. The maximum air velocity is equal to 0.88 m/s and the mass flow rate of air is equal to 185 g/s. Table 6 summarizes the main parameter values.

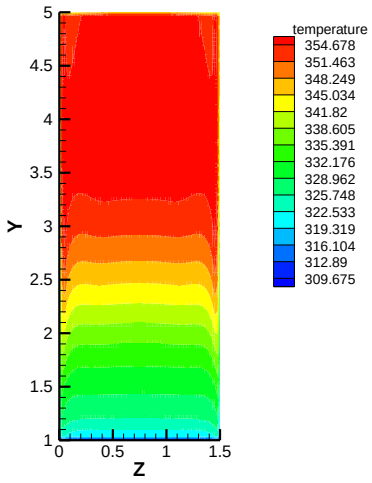

Figure 16. Temperature field vertical surface for parallel walls and q=300 W/m^2.

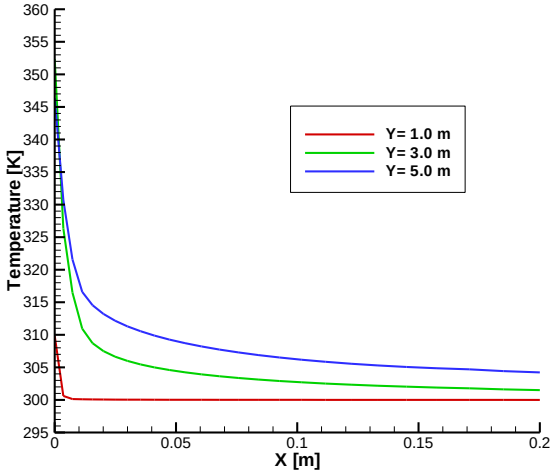

Figure 5. Air Temperature profile in the channel spacing, at the mid-channel section (Z=0.75 m) and several heights for parallel walls and q=300 W/m^2.

Table 6. Values of the significant quantities for parallel walls and q=300 W/m^2.

	H= 1.0 m
Heat flux [W/m^2]	300
Average Nusselt number	52.89
Mass flow rate [g/s]	185
V_{max} [m/s]	0.82
T_{max} [K]	358

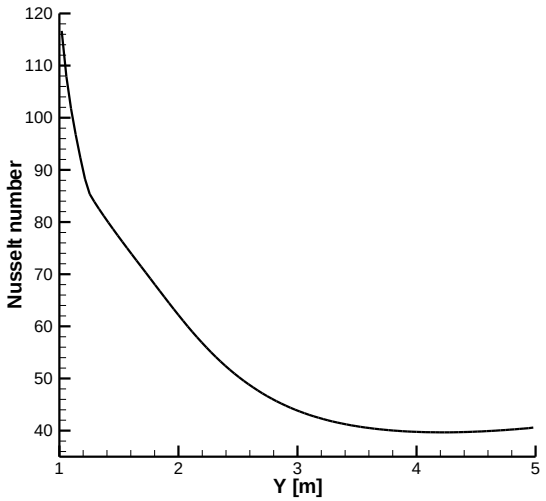

Figure 186. Local Nusselt number on the heated wall, at the mid-channel section (Z=0.75 m) for parallel walls q=300 W/m^2.

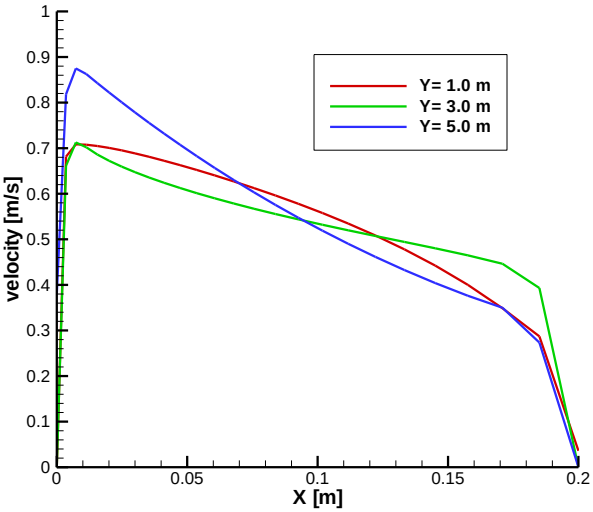

Figure 19. Velocity magnitude profile in the channel spacing, at the mid-channel section (Z=0.75 m) and several heights for parallel walls and q=300 W/m^2.

Comparing the two different geometrical configurations from a thermal point of view, the behavior is similar whereas some changes are related to the fluid dynamic behaviors. In Fig. 20, it is possible to observe that wall temperatures profiles are very similar. While, in Fig. 21, air velocity in the outlet section of converging channel is higher than the one in straight duct.

5. CONCLUSIONS

At an assigned distance from the ground and analyzing the phenomenon for different heat fluxes, is observed an increase of the values of temperature, velocity and mass flow rate with increasing heat flux of wall. Especially doubling the thermal flux, from 300 W/m^2 to 600 W/m^2 there is an increase of almost 30% of the mass flow in the outlet section of the duct; an increase of almost 30% of the maximum velocity of the fluid , and approximately 10% of the maximum temperature of the heated wall.

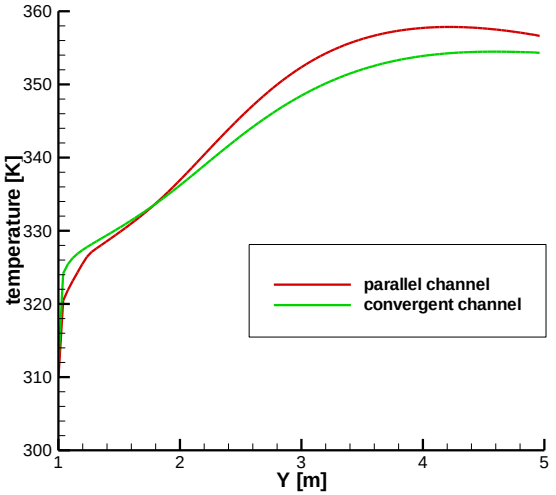

Figure 20. Comparison of centerline heated wall temperature.

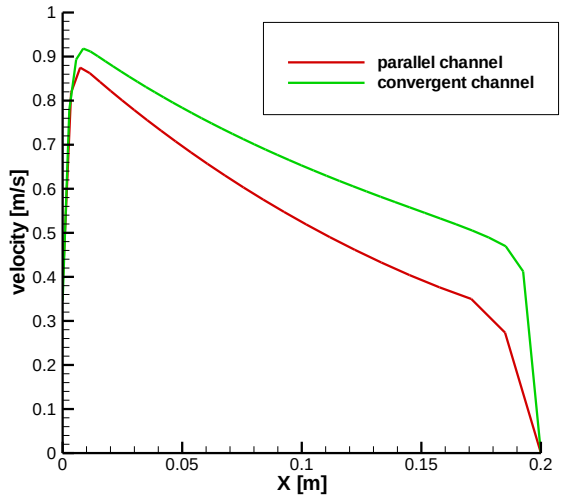

Figure 21. Comparison of outlet magnitude velocity.

The numerical investigation carried out with the purpose of verifying the effect of the geometry of the chimney on the investigated parameters, showed as a straight chimney in place of a convergent does not lead to substantial differences from the thermal point of view and from the investigated fluid. In particular it passes from a maximum speed of 0.92 m/s for the converging channel to 0.88 m/s for the straight duct, therefore a reduction of approximately 5%, while the mass flow is reduced by about 20%, from 227 g/s to 185 g/s.

REFERENCES

1. J. Arce, J.P. Xamán, G. Álvarez, M.J. Jiménez, R. Enríquez and M.R. Heras, A Simulation of the Thermal Performance of a Small Solar Chimney Already Installed in a Building, ASME 2010 4th International Conference on Energy Sustainability, ES 2010 2 , pp. 337-347, 2010.
2. M. Najmi, A. Nazari, H. Mansouri, G. Zahedi, Feasibility study on optimization of a typical solar chimney power plant, Heat and Mass Transfer 48 (3) , pp. 475-485, 2011.
3. A. Asnaghi, S.M. Ladjevardi, Solar chimney power plant performance in Iran, Renewable and Sustainable Energy Reviews 16 (5), pp. 3383-3390, 2012.
4. E. Gholamalizadeh and S. H. Mansouri, A comprehensive approach to design and improve a solar chimney power plant: A special case - Kerman project, Applied Energy 102 , pp. 975-982, 2013.
5. J. Li, P. Guo, Y. Wang, Effects of collector radius and chimney height on power output of a solar chimney power plant with turbines, Renewable Energy 47 , pp. 21-28, 2012.
6. A.Y.K. Tan and N.H. Wong, Parameterization Studies of Solar Chimneys in the Tropics, Energies 6 (1), pp. 145-163 2013.
7. A. Koonsrisuk, T. Chitsomboon, Effects of flow area changes on the potential of solar chimney power plants, Energy 51 , pp. 400-406, 2013.4
8. J. Schlaich, The Solar Chimney: Electricity from the Sun, Edition Axel Menges, Stuttgart, Germany, 1995.
9. W. Haaf, K. Friedrich, G. Mayer, J. Schlaich, Solar chimneys, Part I: principle and construction of the pilot plant in Manzanares, International Journal of Solar Energy 2, pp. 3-20, 1983.
10. M.A. Bernardes, S. Dos, R.M. Valle, M.F.B. Cortez, Numerical analysis of natural laminar convection in a radial solar heater, International Journal of Thermal Science 38, pp. 42-50, 1999.
11. T.W. Von Backström, TP. Fluri, Maximum fluid power condition in solar chimney power plants-an analytical approach, Solar Energy 80, pp. 1417-1423, 2006.
12. T.W. Von Backstrom, A.J. Cannon, Compressible flow through solar power plant chimneys, Journal of Solar Energy Engineering 122, pp. 138-145, 2000.
13. J.P. Pretorius, D.G. Kröger, Critical evaluation of solar chimney power plant performance, Solar Energy 80, pp. 535-544, 2006.
14. T.Z. Ming, W. Liu, G.L. Xu, A.W. Fan, A study of the solar chimney power plant systems, Journal of Engineering Thermodynamics 3, pp. 505-517, 2006.
15. C.B. Maia, A.G. Ferreira, R.M. Valle, M.F.B. Cortez, Theoretical evaluation of the influence of geometric parameters and materials on the behavior of the air flow in a solar chimney, Computers and Fluids 38, pp. 625-36, 2009.
16. T. Tahar, D. Mahfoud, Numerical Simulation of Natural Convection in a Solar Chimney, International Journal of renewable energy, pp. 713-716, 2012.
17. B.E. Launder, D.B. Spalding, The numerical computation of turbulent flow, Comput Meth Appl Mech Eng 3, pp. 269–289, 1974.
18. Fluent Inc. Fluent 6 manuals. Fluent Inc. ed. 2009.